Towards absolutely calibrated ECE Michelson measurements in EC heated plasmas at W7-X

Johan Willem Oosterbeek[1,*], *Mathias* Stern[1], *Neha* Chaudhary[1], *J.F. Guerrero* Arnaiz[1], *Matthias* Hirsch[1], *Walter* Kasparek[2], *Carsten* Lechte[2], *Burkhard* Plaum[2], *Stefan* Schmuck[1], *Torsten* Stange[1], *Matthias* Steffen[1], *R.C.* Wolf[1], and *the* W7-X team

[1]Max-Planck-Institut für Plasmaphysik, Teilinstitut Greifswald, Wendelsteinstraße 1, 17491 Greifswald, Germany
[2]University of Stuttgart, Institute of Interfacial Process Engineering and Plasma Technology IGVP, D-70569 Stuttgart, Germany

Abstract. A Michelson Interferometer is in use at Wendelstein 7-X (W7-X) to probe the Electron Cyclotron Emission (ECE) spectrum [1], [2], [3]. During the past operational campaign (OP2.1), 2^{nd} and 3^{rd} harmonic ECE power density spectra have been routinely recorded in the presence of X2- and O2-mode Electron Cyclotron Resonance Heating (ECRH). However, combination of the particular notch filter arrangement and high transmission line losses have thus far prevented overall calibration using a hot source - cold source exposure at the input antenna. As an alternative, the response of the individual components is measured and summed. While reasonable numbers on electron temperature are obtained in X2-mode polarisation, interaction between front-end components is neglected and large error bars must be assumed. But the information on the individual components, together with synthetic modelling and data from experiment (OP2.1), has been used to design a new front-end with improved S/N. This optimisation is discussed in this paper with focus on notch filter selection, a new transmission line (Tx-line) and a novel combined quasi-optical taper / polarizer tuner.

1 Introduction

Michelson Interferometers scan the plasma microwave spectrum over several ECE harmonics. If the plasma is optically thick, the emitted power is a measure for the electron temperature [4]. By relating the emission frequency to the local magnetic field, an electron temperature profile is obtained. For calibration a black body source at two different temperatures is used. This signal is very low compared to the plasma signal and is further decreased by Tx-line losses. Coherent averaging is used to recover the temperature step at the output of the detector, but practical issues limit extreme integration times. This paper describes Tx-line losses and deformation of the spectrum by ECRH and notch filters.

2 Michelson Interferometer and implementation at W7-X

2.1 Principle of operation

A Michelson is a Fourier transform spectrometer in which the RF input signal is combined with a phase-shifted copy of itself by means of a movable mirror that provides an optical path difference x. The envelope of the modulation is the interferogram and shows minima and maxima as a function of phase shift and frequency. When expressed by wavenumbers $\sigma = \lambda^{-1}$, the interferogram $I(x)$ from a black body RF input signal $W(\sigma)$is [5]:

$$I(x) = \int_0^\infty W(\sigma)\cos(2\pi\sigma x)d\sigma \qquad (1)$$

A reverse Fourier transform on the cosine transform of eq. 1 resolves the wavenumbers, i.e. the spectrum, again. The W7-X Michelson interferometer is used in the frequency range of 100 ... 300 GHz and has a maximum mirror peak-to-peak amplitude of 16 mm that gives a spectral resolution of $\approx$ 5 GHz [1]. The mirror frequency is 22 Hz, in which there is one stroke forth and one stroke back, giving an interferogram each 23 ms. In practice only one stroke is used, setting the temporal resolution to 45 ms. The detector is an InSb bolometer cooled to LiHe temperature. From previous data sheets [6] and literature [7] the NEP is around 10^{-13} W Hz$^{-0.5}$.

A simulated typical W7-X ECE spectrum, generated by TRAVIS [8], is shown in Fig. 1. Input for the simulation are a toroidal field of 2.5 T and simple quadratic profiles for temperature (T_e) and density (n_e), with central T_e = 2 keV and central $n_e = 0.8\times10^{19}$ m^{-3}. The Michelson is set to X-mode, giving directly $T_{rad} = T_e$ in the 2^{nd} harmonic.

To analyse the instrument response a model is developed that takes an arbitrary spectrum, performs the cosine transform using the instrument parameters and subsequently

*e-mail: hans.oosterbeek@ipp.mpg.de

[1]An instrument paper addressing issues as frequency range, spectral resolution, NEP and overall S/N is being drafted by the authors.

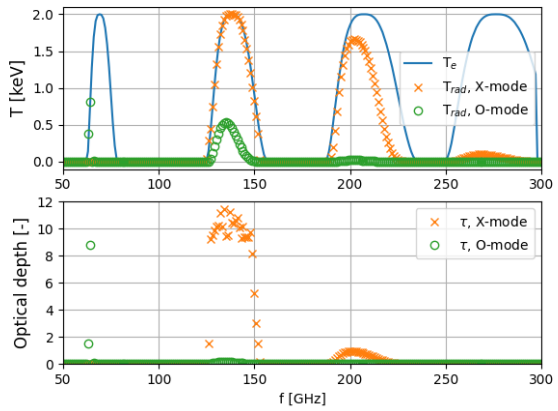

Figure 1. Typical W7-X ECE spectrum calculated with TRAVIS. Top: blue traces show the electron temperature (T_e) in the 1^{st}, 2^{nd} , 3^{rd} and 4^{th} harmonic while the orange and green traces show the actual emission by the plasma labeled T_{rad}. In the lower plot the optical depth for either mode is shown.

performs the inverse Fourier transform. For illustration a simulation is shown in Fig. 2 for the 2^{nd} and the 3^{rd} harmonic as in Fig. 1, using a mirror excursion of 16 mm.

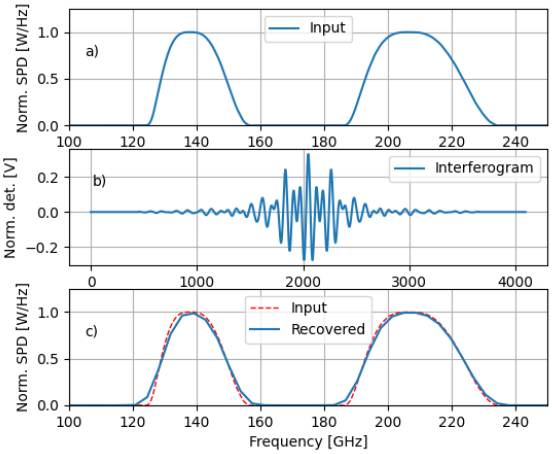

Figure 2. Simulated instrument response: a) input spectrum, b) interferogram, and c) recovered spectrum. Despite a rather poor spatial resolution of 5 GHz the Gaussian shaped spectrum is well recovered, as expected for a Gaussian shaped function.

2.2 Front-end and ECE power

A simplified arrangement of signal transmission from plasma to the input of the interferometer with focus on losses, is shown in Fig. 3. The individual component losses were measured using a black body source and the Michelson and summed are of the order of 20 dB. For a known plasma temperature T_{PL} this number is also found by scaling the corresponding detector voltage V_{PL} with a local calibration at temperature T_{HS} and detector voltage V_{HS}, and then accounting for the linear losses L giving:

$$T_{PL} = \frac{T_{HS}}{V_{HS}} V_{PL} L \tag{2}$$

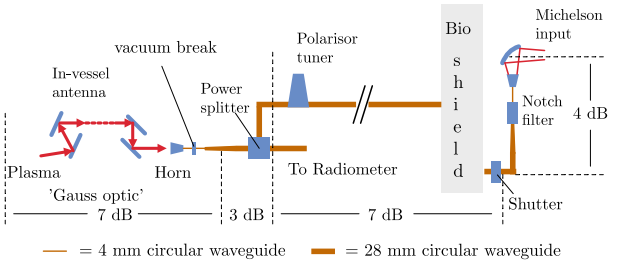

Figure 3. Simplified schematic of the RF-section between plasma and the input of the instrument, with focus on losses.

Despite the high front-end losses reasonable spectra from the plasma are acquired. But the losses are too high for calibration by two practical black body sources at different temperatures: 'hot' and 'cold' in front of the antenna. It has been demonstrated that local calibration with a black body source at liquid Nitrogen (LN2) temperature versus a black body source at 600°C provides good difference spectra, using coherent averaging for order 40 minutes to improve the S/N [9], [10]. This amounts to approximately 30000 averages for each source (taking one interferogram per round mirror trip), which gives an improvement in S/N by ≈ 175. But inclusion of the front-end losses results in integration times of the order of days during which environmental variables such as temperature, air humidity, electrical interference and stability of the electronics affect the averaging. And there are practical issues as attending the set-up and refilling LN2.

The above experience is in broad agreement with a simple consideration of the overall instrument S/N (to be followed up by footnote on page 1). The radiated intensity of an optically thick plasma, or that of a black body calibration source, is given by the Planck function in units of W per solid angle per unit bandwidth per mode of radiation. By illuminating the full antenna aperture and by using the Raleigh-Jeans approximation, the power coupled to the antenna per mode can be approximated by kT_eB [7], where k is the Boltzmann constant, T_e electron temperature and B bandwidth. The power in the 2^{nd} harmonic as in Fig. 2, with T_e = 2 keV, is then of the order of 5 μW when taking a top-hat profile from 130 to 150 GHz and assuming a single mode entering the interferometer (Sec. 2.4). When accounting for 20 dB loss it is order 50 nW at the detector. Assuming a NEP of $1{\times}10^{-13}$ W $Hz^{-0.5}$, over 20 GHz, the noise power would be of the order of 15 nW. Fig. 4 shows uncalibrated spectra as a function of time for pulse 20230215-032, with T_e (300 s) = 2.3 keV and using a notch filter at 140 GHz.

2.3 Stray radiation

Stray radiation is caused by non-absorbed gyrotron power and may be magnitudes larger than the ECE signal. ECRH

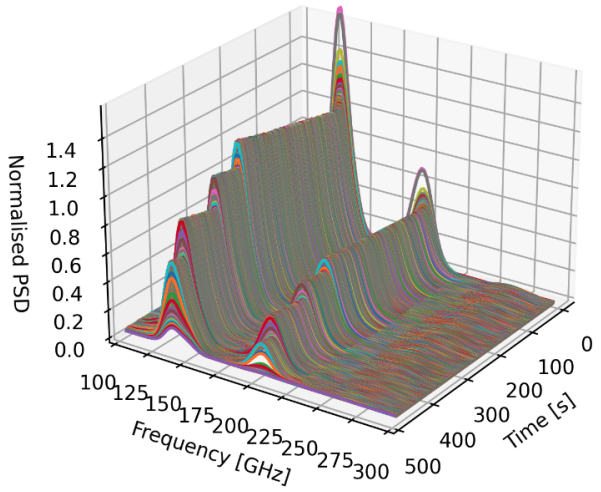

Figure 4. Instrument potential showing uncalibrated spectra for 2^{nd} and 3^{rd} harmonic ECE, # 20230215.032 with notch filter at 140 GHz. A notch @ 140 GHz GHz is not obvious from the data but note that notch depth and the ECRH line are competing effects, the instrument resolution is broad and that the ECE peak is normally not at the ECRH line.

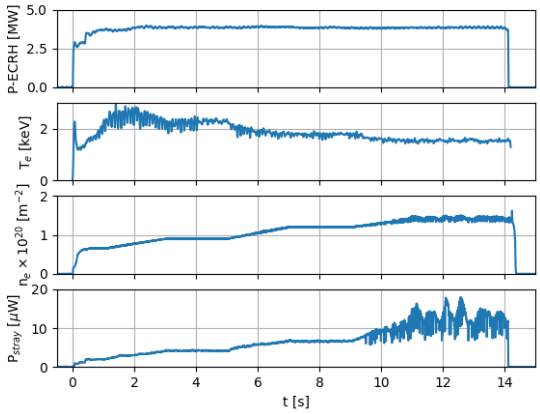

Figure 5. Stray radiation as measured with a Schottky-diode in front of the Michelson without a notch filter. Discharge 20230315-047 with 5 MW O2-mode ECRH. The lower plot shows a steady increase in stray radiation as the electron temperature falls due to increasing density.

absorption in X2 heating is very high, but in O2 and X3 heating noticeably lower, however, W7-X high density operation does require O2 and X3 schemes. In Fig. 5 a plot is shown of a robust single mode (D-Band) Schottky diode replacing the Michelson interferometer. Given the high front-end losses ECE cannot be detected at this location by the diode and the signal is gyrotron power only. In the pulse 5 MW of O2 ECRH was used with a density ramp, giving rise to increasing levels of stray radiation as the electron temperature decreases. Up to about 9.5 seconds there is a steady stray radiation signal, after that strong fluctuations set in, typical for standing waves in a metal cavity. The diode was calibrated using a low power source and a power meter. Maximum stray radiation levels of 15 μW were measured. The diode was mounted just before the notch filter (Sec. 2.4), at which location the front-end losses are estimated to be 17 dB. Projecting the measured signal power to the antenna input in the vessel one finds around 0.8 mW. Assuming the 4-mirror Gaussian beam antenna of the front-end (Fig. 3) receives only one mode - and considering the diode is a single mode detector - the antenna effective aperture is λ^2 at 140 GHz. This suggest a stray radiation level of order 200 Wm^{-2}, for this pulse as coupled to the antenna in module 4 where the ECE antenna is located.

The InSb-bolometer in the Michelson is fairly robust, it can take several tens of mW of power before damage occurs [11], but the problem is that the interferogram will be dominated by stray radiation and that the ECE spectrum can not be extracted. This is visualised by taking the normalised 2^{nd} harmonic spectrum as in Fig.2, and assuming a gyrotron line from 139.9 to 140.1 GHz with as amplitude the ratio of gyrotron power over ECE power = 15 μW/50 nW = 300. Note that 50 nW is the ECE power over the 20 GHz wide top-hat band and not the ECE power in the band 139.9 to 140.1 GHz, which would result in a ratio of 30000. For visualisation the ratio 300 is taken as the recovered spectrum is still instructive. In Fig. 6 it is seen that the interferogram is dominated by stray radiation, that the recovered spectrum is a factor 10 larger as the ECE spectrum but is narrower and centered around 140 GHz.

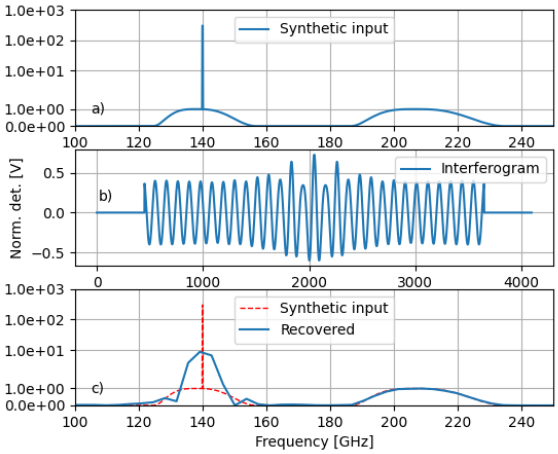

Figure 6. Modeled instrument response of a synthetic ECE spectrum with a 140 GHz gyrotron line (note: log scale). The recovered ECE spectrum is completely dominated by the gyrotron line, which is much broadened by the limited spectral resolution of the instrument (Section 2.1 and footnote 1).

2.4 Notch filter

The notch filter is required to remove stray radiation power from the gyrotrons, principally that of the ECRH system at 140 GHz but in future also that of the 174 GHz CTS probing beam [12], [13]. A Michelson classically has a

large aperture and oversized detector such that multiple modes are collected, improving S/N. This requires a multi-mode single notch filter but otherwise in transmission over the full band band (100 ... 300 GHz). Several prototypes have been developed [1], [14] but insertion losses, reproducibility, alignment, and broad notches as well as satellite notches remain big challenges. As an alternative approach a single mode notch filter has been used during OP2.1 at the expense of signal power. Noting however, that the Gauss-optic and antenna pattern are optimised for focus in plasma and only allow a limited number of modes (considered 1 in the calculation example in Section 2.3). Fundamental mode notch filters are well developed and can provide deep notches of only a few 100 MHz wide. The data in Fig. 5 can readily be used to find a realistic notch depth. Taking a 2 keV plasma and ECE power in a bandwidth comparable to the gyrotron power, one finds 64 nW, or -42 dBm at the antenna. At the input of the Michelson it is -63 dBm. The gyrotron power before the notch filter is at 15 μW or -18 dBm, at the input of the receiver it is 4 dB less, i.e. at -22 dBm. Requesting $P_{ECE} = P_{gyrotron}$ one finds a notch of 63 - 22 = 41 dB. It is prudent to request the gyrotron power to be a factor 10 lower as the ECE power, in such case a notch depth of 51 dB.

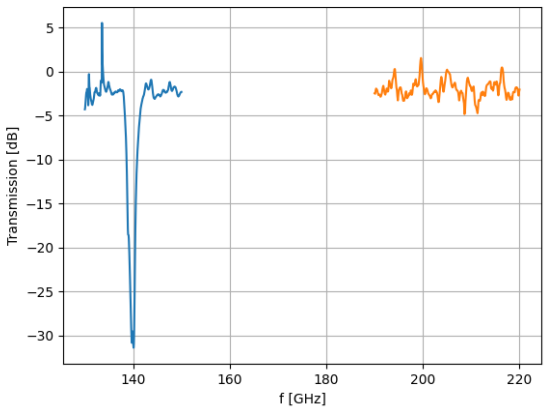

Figure 7. Transmission of the notch filter as used in OP2.1. Insertion losses are very modest. But the notch (30 dB) is too low for O2-heated plasmas and the notch width should be much decreased. Transmission for the 3^{rd} harmonic for this type of design is very good.

During OP2.1 a single mode cavity notch filter in F-Band [15] was available with characteristic as shown in Fig. 7. Measurements in X2 provided genuine ECE - given the notch of 30 dB and a notch-free band around the 3^{rd} harmonic - but with a large void around the gyrotron frequency. The impact of the notch on a recovered spectrum was investigated by placing the notch from 137.5 $\cdots$ 142.4 GHz in the normalised synthetic ECE spectrum of Fig 2: see Fig. 8. It is seen the 2^{nd} harmonic is now lower in amplitude and there is a flattening at the location of the notch.

The loss of power due to the transition to single mode at the notch filter was assessed experimentally and is shown

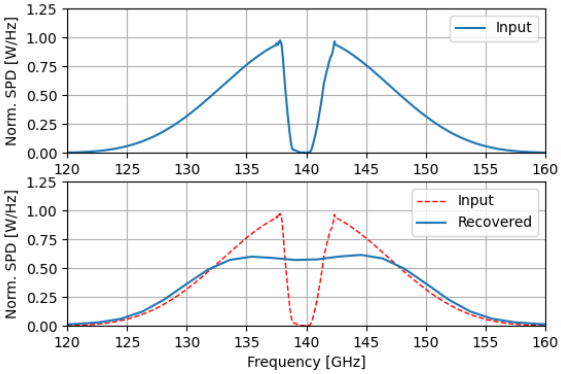

Figure 8. Insertion of the notch filter (range 137.5 dB $\cdots$ 142.4 GHz) in the synthetic 2^{nd} harmonic ECE spectrum as shown in Fig. 2. The recovered spectrum is seen to be flattened and broadened. NOTE that in the synthetic input spectrum NO ECRH line is included in this example.

in Fig. 9. The Tx-line is circular 28 mm waveguide, but is contains a 4 mm section at the vacuum window.

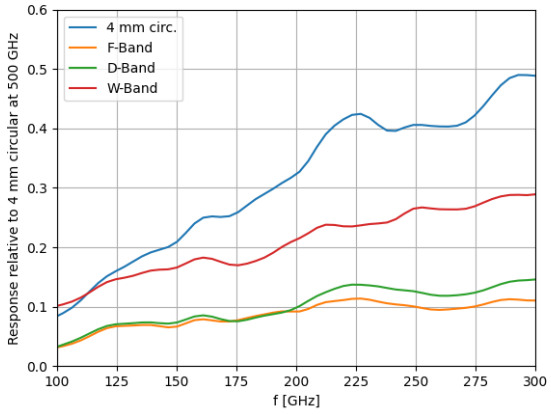

Figure 9. Michelson response to a black body source at elevated temperature for 4 different size waveguides at the input. A 4 mm circular waveguide supports up to 9 modes at 140 GHz [16], while fundamental D-band only supports one mode. Still, the difference in signal output as measured is only order 4 dB. The working hypothesis is that the Michelson front-end optics support only a limited number of higher order modes.

To demonstrate operation as well as shortfall of the present notch filter, the Michelson response to pulse 20230314.065 is shown in Fig. 10. It shows top to bottom: heating power, central temperature, line integrated density and Michelson spectra at different times into the discharge. The X2 ECE cutoff is at $n_e = 1.2{\times}10^{20}$ m^{-3}, starting at about 5.5 s. The first spectrum shown is at 2.0 s: no cut-off and low stray radiation. From 6.0 s to just over 6.5 s, O2-heating is applied causing very large stray radiation due to low electron temperature $\rightarrow$ low optical depth. A spectrum at 6.5 s shows the peak in the spectrum has shifted to 140 GHz but with negligible shift in the 3^{rd} har-

monic. The 2^{nd} harmonic is also very large despite the cut-off. A subsequent spectrum, at 6.6 s, just after ECRH switch off, shows a very much lower amplitude, the peak has moved back to 140 GHz and the signal is asymmetric due to the ECE X2 cut-off. It is concluded that the spectrum at 6.5 s is the instrument response to stray radiation and NOT to ECE, while the other two spectra do show the instrument response to ECE.

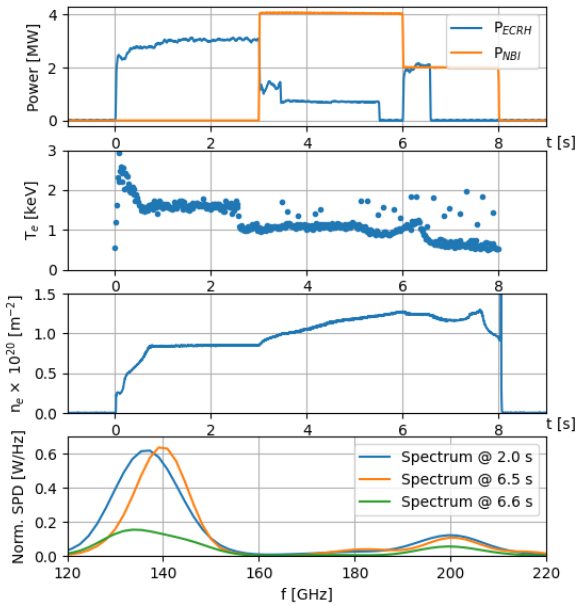

Figure 10. Response to pulse 20230314.065. The first spectrum, at 2.0 s, is X2 heating and no cut-off: spectrum fine. From 6.0 s to 6.5 s there is O2-mode heating with low T_e and very high stray radiation. But the spectrum (@ 6.5 s) shows a high temperature and is shifted to 140 GHz. At 6.6 s the ECRH is off, 2^{nd} harmonic ECE in cut-off: the peak in the spectrum moves back and the amplitude is very low. It is concluded the the spectra at 2.0 s and at 6.6 s show ECE while the spectrum at 6.5 s is saturated by ECRH. (Notch filter from Fig. 7 used).

3 Development work

The large front-end losses pose a problem for calibrating the homodyne InSb-detector and work is ongoing to reduce these losses. The initial measures described in this section aim to reduce the overall losses by 6 dB to 10 dB. A concept for new notch filter arrangement is discussed.

3.1 Waveguide diameter and number of components

The current Tx-line and waveguide components, such as mitre bends and polarisor tuners, are in 28 mm diameter circular waveguide. Mode conversion losses in these components contribute significantly to the overall losses as they scale as $(\lambda_0/a)^{3/2}$ with a the waveguide radius and λ_0 the vacuum wavelength [17]. These losses tend to dominate Ohmic losses that scale with waveguide length. A replacement of the section of waveguide from the power splitter up to and including the biological wall penetration (see Fig. 3) is ongoing using a 70 mm diectrically lined circular waveguide. A new routing of the section, exploiting a recent relocation of the Michelson closer to the in-vessel antenna, reduces the number of mitrebends in addition. The dielectrically lined waveguide [18] has been kindly received from Stuttgart University [20], and stems from development work towards a broad band telecommunication network using oversized waveguide, before the era of optical fibre availability. The lining is Al_2O_3 with thickness 66 μm. The larger diameter cuts mode conversion losses and these waveguides support the HE11 mode, which more efficiently couples to the Gaussian modes in the various components, compared to the TE11 mode propagation in pure metallic waveguides. Therefore, below the $\lambda/4$ - resonance of the dielectric lining (corresponding theoretically to 380 GHz), good transmission performance is expected. Such waveguides have also attracted recent attention in the THz region [19].

3.2 Polarisation tuner

A further reduction of mitrebends is made by replacement of the waveguide polarisor tuner with a quasi-optical polarisation tuner. This tuner is required to align the E-vector of the X-mode emission from the plasma to the orientation of the wire polarisor grid in the interferometer. In a novel development by Stuttgart University [20] the polarisor tuner is combined with a taper from 70 to 28 mm waveguide to connect to the remaining section of 28 mm circular waveguide. A sketch of the polarisor tuner is given in Fig. 11.

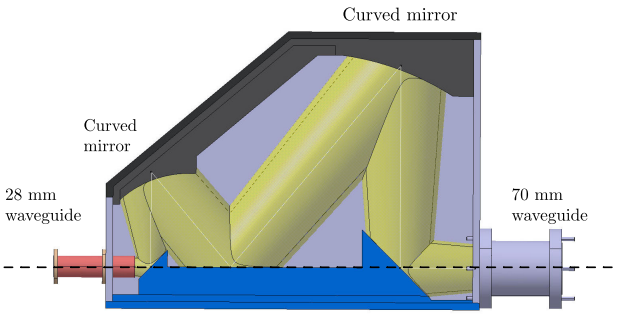

Figure 11. Polarisor tuner combined with taper. The dotted line shows the axis of rotation, which will rotate the E-vector at the input waveguide to any projection into the output waveguide. The curved mirrors taper from 28 to 70 mm waveguide.

3.3 Notch filter

The main challenge for the notch filter is the requirement of a single notch of very high quality in a broad spectrum. But in microwave engineering mostly frequency bands are used with wavelength and component sizes matched to favourable ratios. The relevance with respect to the notch filters became clear during the work by Goll [14] and Cu Castillo [10]. One could in the most simple case define a

low-pass band from 100 to 170 GHz and a high-pass band starting at 180 GHz. The low-pass band has a fundamental notch filter at 140 GHz and the high-pass band could in principle do without notch filters, as long as there is large isolation between the bands (e.g. no 140 and 174 GHz leakage into the high-pass band). Both bands are then combined again in quasi-optics and are fed as a single beam into the interferometer. Preliminary work on such a concept in quasi-optical design is in progress at Stuttgart University [20]. A possible notch filter at 140 GHz could then e.g. be a design by D. Wagner [21] providing a narrow and deep notch at 140 GHz, but without requirements for passing the 3^{rd} harmonic. Such a filter was in fact gratefully used with the Michelson during a number of experiments.

4 Summary

The Michelson interferometer has been operated with a fundamental mode notch filter during W7-X operational campaign OP2.1. This enabled routine recording of 2^{nd} and 3^{rd} harmonic ECE spectra during X2 heating schemes. But the S/N of the system is too low to allow absolute calibration using a hot source at the in-vessel antenna, despite using coherent averaging. The front-end losses have been analysed and are around 20 dB. Here a large reduction in losses is believed possible. As a first phase a large section of transmission line and components in 28 mm diameter is being replaced with 70 mm diameter waveguide and components. A planned second phase is a dedicated antenna for the Michelson, gaining 3 dB instantly as the antenna is no longer shared with the radiometer, and addressing the not well understood 7 dB insertion loss left of the vacuum break as measured with the Michelson. During experiments with O2 ECRH heating sometimes too much stray radiation entered the receiver and the notch depth should be increased from 30 to 55 dB. Also the notch width must be reduced from 1.5 GHz to several 100 MHz only. The reduction in S/N by passing only one propagation mode from plasma to detector, as a caveat with a fundamental mode notch filter, is in practice limited to around 4 dB. A new scheme for the notch filter, using division and recombination in RF-bands, is under investigation and offers inclusion of a notch filter at 174 GHz for CTS operation.

This work has been carried out within the framework of the EUROfusion Consortium, funded by the European Union via the Euratom Research and Training Programme (Grant Agreement No 101052200 - EUROfusion). Views and opinions expressed are however those of the author(s) only and do not necessarily reflect those of the European Union or the European Commission. Neither the European Union nor the European Commission can be held responsible for them.

References

[1] N. Chaudhary et al., Journal of Instrumentation 15 P09024.

[2] J.W. Oosterbeek et al, Fusion Engineering and Design, Volume 146, Part A, September 2019

[3] J.W. Oosterbeek et al, Proceedings of the 49th Conference on Plasma Physics of the European Physical Society (EPS), Bordeaux, France, July 3rd to 7th.

[4] M. Bornatici *et al*. Electron cyclotron emission and absorption in fusion plasmas. *Nucl. Fusion* **23** (1983) p. 1153

[5] S.P. Davis et al., 'Fourier Transform Spectroscopy', Academic Press 2001

[6] QMC Instruments, 'Operating instructions for Fast InSb Detector system, Type QFI/3, Serial No: 1100

[7] H-J. Hartfuss and T. Geist, 'Fusion Plasma Diagnostics with mm-Waves', Wiley-VCH, 2013

[8] N. Marushchenko *et al*. Computer Physics Communications, Volume 185, Issue 1, January 2014, Pages 165-176

[9] N. Chaudhary, 'Investigation of optically grey electron cyclotron harmonics in Wendelstein 7-X', Ph.D Thesis, Berlin 2021

[10] H.I. Castillo, 'Extension of the operational capabilities of the Martin-Puplett Michelson Interferometer at W7-X', M.Sc Thesis, Greifswald, 2022

[11] J. Cox, QMC Instruments Ltd. School of Physics and Astronomy, Cardiff University, Private communication.

[12] S. Ponomarenko et al., 'Development of the 174 GHz collective Thomson scattering diagnostics at Wendelstein 7-X', Rev. Sci. Instrum. 95, 013501 (2024)

[13] D. Moseev et al., Commissioning and first results of the 174 GHz collective Thomson scattering diagnostic at Wendelstein 7-X, Journal of Instrumentation 19(03):C03056

[14] M. Goll, 'Towards a 140 GHz Notch Filter for Wendelstein 7-X Broadband ECE Diagnostics', B.Sc Thesis, Berlin, 2022

[15] A. Krämer-Flecken et al., Fusion Engineering and Design, 56-57 (2001) 639-643

[16] Nikitin et al., Proceedings of the 2011 IEEE International Symposium on Antennas and Propagation (APSURSI), 3-8 July 2011, Spokane, WA, USA

[17] M.K. Thumm et al., 'Passive high-power microwave components', IEEE Transactions on plasma science, vol. 30, No. 3, June 2002

[18] M. Krahn, Aluminium waveguide with aluminium oxide dielectric lining', Felten & Guilleaume Carlswerk AG, Nachrichtentecnik, ntz Archiv Bd.2 (1980) H. 1

[19] K. Thackston et al., 'Dielectric Lined Waveguides for Low Loss Millimeter Wave and Terahertz Transmission, DOI: https://doi.org/10.21203/rs.3.rs-2206864/v1

[20] W. Kasarek, C. Lechte and B. Plaum, Institute of Interfacial Process Engineering and Plasma Technology IGVP, Stuttgart University.

[21] D. Wagner et at., 'Single- and Two-Frequency Sub-THz Waveguide Notch Filters With Rejection Frequencies Within and Beyond the Passband, IEEE Transactions on Microwave Theory and Techniques, vol. 71, no. 6, pp. 2558-2566, June 2023